Possibilities for Improved Supersonic Inlet Performance

Norman E. Sorensen* and Daniel P. Bencze*
NASA Ames Research Center, Moffett Field, Calif.

The results from detailed large-scale inlet tests were examined to assess the penalties, in terms of vehicle cruise range, for boundary-layer bleed, less than ideal engine-face pressure recovery, inlet weight, and external cowl drag. The assessment suggested specific improvements in the design of the inlet system that may increase the range of a typical supersonic transport approximately 6.9%. While no single design improvement can account for a large increase in range, careful attention to each design detail can yield a substantial total improvement. Because of noise considerations, future engines for advanced supersonic transports may be approximately 50% larger than used for the present study, making the effects of improved inlet performance even more important.

Nomenclature

A_c = capture area
c_p = pressure coefficient per unit width
D = capture diameter
M = Mach number
m = mass flow
m_L = capture mass flow, $\rho_L U_L A_c$
p = static pressure
p_t = total pressure
$\bar{p}_t$ = area-weighted average total pressure
U = velocity
w = louver width
x = longitudinal station
α = angle of attack
δ = ratio of engine-face total pressure to standard sea-level static pressure
θ = ratio of freestream total temperature to standard sea-level static temperature
ρ = density
ϕ = angle

Subscripts

bl = bleed
c = cowl
CRIT = critical
L = local
max = maximum
min = minimum
OP = operating
r = bleed exit ramp
$v.v.$ = vortex valves
2 = engine face

Introduction

WHEN considering the efficiency of long range supersonic cruise vehicles such as supersonic transports, the performance penalties associated with the engine inlet system can account for 10–20% loss in aircraft range. Improvements in the performance of the inlet system, therefore, can significantly increase the over-all performance of the vehicle. In this paper the results from tests of two large-scale inlet systems[1–3] (50 cm capture diam) are compared. The comparison shows what improvement in performance has already been achieved in terms of cruise range of a typical long range cruise vehicle.[4] The assessment includes penalties for the boundary-layer bleed system, engine-face pressure recovery, inlet weight, and external drag. The main objective is then to show what further improvements can be made in the design of the inlet system and the corresponding potential benefits in cruise range.

Large-Scale Tests

Inlets

The test results from two similar axisymmetric inlet systems, designated N_5[1] and P[2,3] in Fig. 1, have been studied. These inlets differ mainly in the bleed-system design and the method used to achieve the control margin (to be discussed later) necessary to prevent the inlets from unstarting from sudden internal or external flow disturbances. One other important difference is the incorporation of cowl-throat doors in the N_5 inlet that "hinge" in the supersonic diffuser and extend nearly to the engine face. With the centerbody extended to the transonic position these doors provide increased transonic airflow when rotated radially outward about the door hinges (dashed line). However, the doors represent a weight penalty which is traded for increased transonic airflow and can be an important requirement (not included in the P inlet) depending on the engine cycle selection.† Aside from different intermal contours, other major differences include the use of a centerbody boundary-layer control scoop on the N_5 inlet and also the eight vortex valves to provide the required control margin which will be discussed later.

Both inlets use a "traveling centerbody bleed system" for proper boundary-layer control in the throat during off-design operation. This system consists of a series of bleed compartments which vent through fixed ports in the centerbody support tube, which in turn vent to the centerbody bleed exit louvers through the hollow support struts (see Fig. 1). The system maintains centerbody throat bleed opposite the cowl-throat bleed as the centerbody is translated forward for off-design started operation. Such a traveling bleed system is usually required for axisymmetric inlets designed for high transonic airflow because the inlet throats remain fixed relative to the cowl as the centerbody is translated forward. That is, the centerbody bleed must be opposite the cowl bleed, a condition which the traveling bleed system provides.

Details of the N_5 and P inlet bleed systems are shown in Figs. 2 and 3, respectively. The centerbody positions correspond to the cruise conditions of $M = 2.65$ and $\alpha = 0°$. For the N_5 inlet all the bleed holes on both the cowl and centerbody are slanted forward 20° relative to the local

Presented as Paper 73-1271 at the AIAA/SAE 9th Propulsion Conference, Las Vegas, Nev., November 5–7, 1973; submitted November 26, 1973; revision received March 8, 1974.

Index category: Airbreathing Propulsion, Subsonic and Supersonic.

*Research Scientist. Member AIAA.

†For example, an afterburning turbojet may require more transonic airflow than an unaugmented turbojet which can be trimmed more to match the inlet airflow supply at transonic speeds.

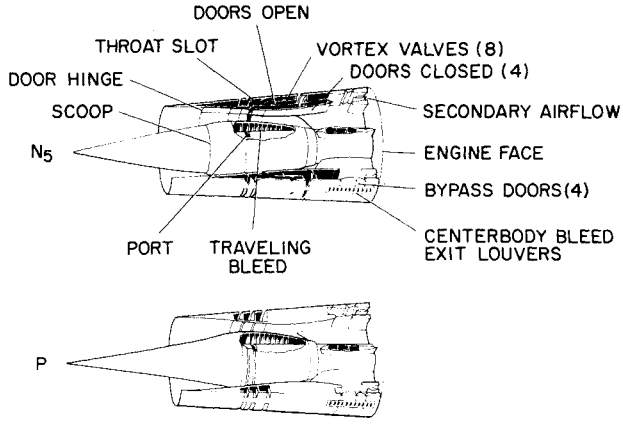

Fig. 1 Inlet systems, cruise geometry.

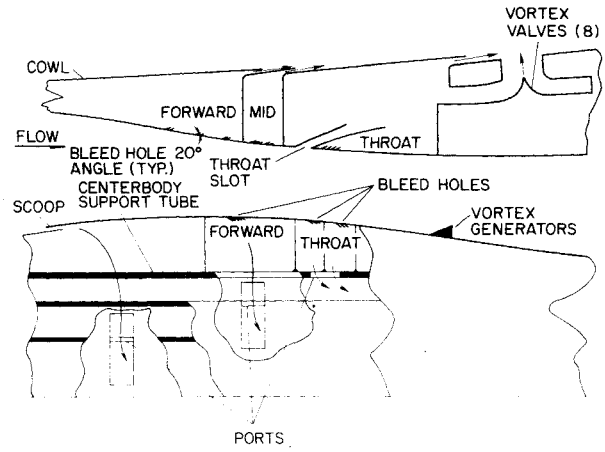

Fig. 2 Bleed system, N_5 inlet, $M_L = 2.65$, $\alpha = 0°$.

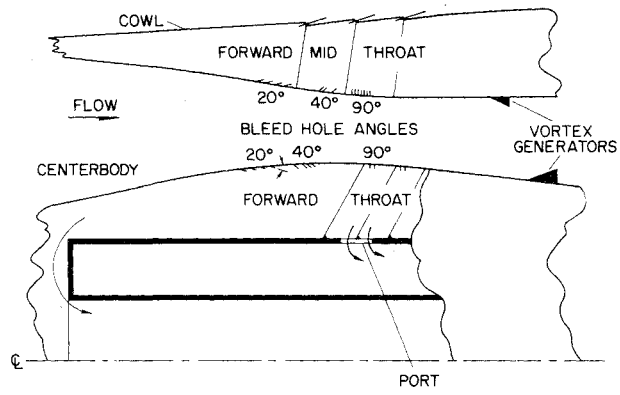

Fig. 3 Bleed system, P inlet, $M_L = 2.65$, $\alpha = 0°$.

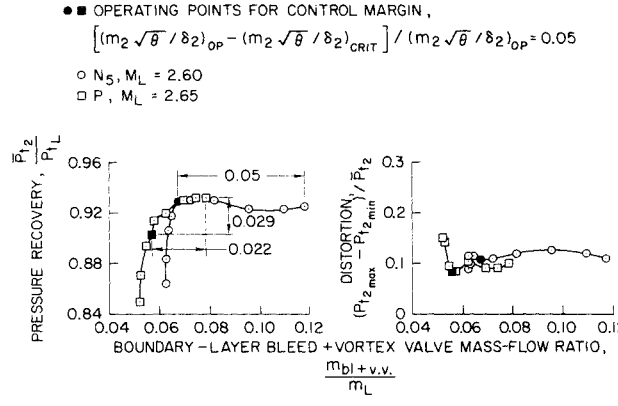

Fig. 4 Cruise performance, $\alpha = 0°$.

surface to maximize the total-pressure recovery in the bleed plenum chambers, thus minimizing the total-momentum drag of the overboard bleed flow. Three separate plenum chambers (forward, mid, and throat) are provided on the cowl and centerbody to prevent boundary-layer separation caused by recirculation of the high pressure downstream bleed flow into the main duct flow through the low pressure upstream bleed regions. In addition, compartmentation increases the average plenum chamber pressure recovery. The cowl bleed flow is exited through louvered nozzles designed to fully expand the flow to obtain minimum drag. The centerbody bleed flows (scoop, forward, and throat) pass through three separate ducts in the centerbody support structure and then are exhausted overboard through louvered full-expansion nozzles. A throat slot is located on the cowl just upstream of the position of the terminal shock wave system. When minor airflow variations cause the terminal shock wave to move forward and tend to unstart the inlet, the pressure in the throat slot increases sharply, destroys the swirl flow in the vortex valves and allows airflow from the main duct to be bypassed overboard. The required control margin is then provided and prevents the inlet from unstarting. Vortex generators are located on the centerbody just downstream of the throat to reduce the airflow distortion at the engine face.

For the P inlet, only the holes in the supersonic diffuser upstream of the throat are slanted forward (20° and 40° relative to the local surface). Normal holes are used in the throat region to help provide the necessary control margin. Instead of using vortex valves to achieve the required control margin, the P inlet uses a combination of increases in both engine-face pressure recovery and bleed flow as the terminal shock wave moves forward from its operating position. In this case, the normal bleed holes in the throat region allowed greater bleed flow-rates than slanted holes when subjected to the high pressure downstream of the terminal shock system. The plenum chambers of the bleed regions were compartmented and the flows were exhausted overboard in a similar manner as for the N_5 inlet except that the centerbody used only two separate centerbody plenums (forward and throat) instead of three. Vortex generators also were located just downstream of the throat on the cowl as well as the centerbody for more effective control of the airflow distortion at the engine face.

Inlet Performance

To compare the performance of the two inlets on a consistent basis, the comparison must be made at the operating point of each inlet where the required control margin exists. In this case the control margin is defined as the ability of the inlet to provide 5% decrease in engine-face corrected airflow (as shown in Fig. 4) without unstarting or requiring a change in geometry. For the cruise condition, the engine-face pressure recovery and distortion for both the N_5 and P inlets are plotted in Fig. 4 as a function of the boundary-layer bleed mass-flow ratio for nearly the same Mach number. For the N_5 inlet bleed mass-flow ratio includes the mass-flow ratio through the vortex valves. The operating points are designated by the filled symbols and include not only the 5% control margin but also a tolerance of 0.05 decrease in local Mach number before the inlet unstarts. The pressure recovery curves illustrate how the control margin is achieved for each inlet. For the N_5 inlet the operating point is at the maximum pressure recovery of 92.8% and requires 6.7% bleed mass-flow ratio. When the terminal shock wave moves upstream from the operating position the vortex valves pass 5% of the engine-face corrected airflow, and provide the

COWL PLENUM	m_{bl}/m_L		$P_{t_{bl}}/P_{t_L}$	
	N_5	P	N_5	P
FORWARD	0.007	0.010	0.132	0.190
MID	0.010	0.009	0.241	0.172
THROAT	0.018	0.014	0.374	0.194
VORTEX VALVES	0.004	—	—	—
CENTERBODY PLENUM				
SCOOP	0.011	—	0.109	—
FORWARD	0.010	0.013	0.154	0.111
THROAT	0.011	0.011	0.347	0.217
$\Sigma m_{bl}/m_L$	0.071	0.057		

Fig. 5 Operating bleed flow and recovery, $M_L = 2.65$, $\alpha = 0°$.

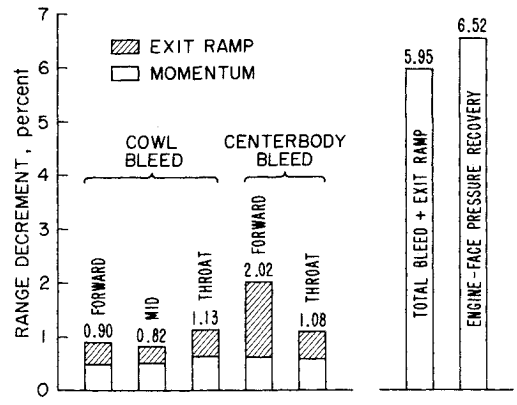

Fig. 7 Cruise range penalties, P inlet, $M_{\text{cruise}} = 2.70$, $\alpha = 0°$.

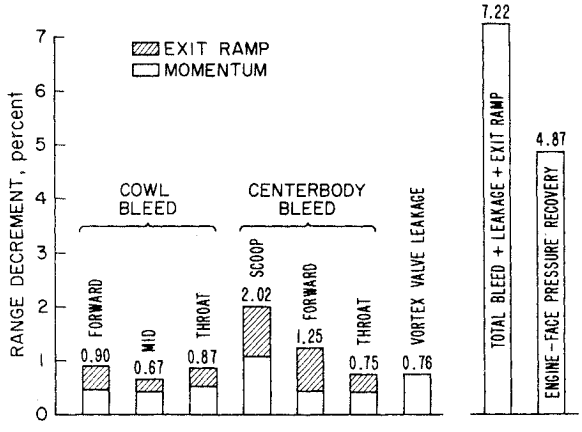

Fig. 6 Cruise range penalties, N_5 inlet, $M_{\text{cruise}} = 2.70$, $\alpha = 0°$.

		RANGE, percent
COWL BLEED	FORWARD	0
	MID	-0.15
	THROAT	-0.26
CENTERBODY BLEED	SCOOP	2.02
	FORWARD	-0.77
	THROAT	-0.33
LEAKAGE	VORTEX VALVES	0.76
	ENGINE-FACE PRESSURE RECOVERY	-1.65
WEIGHT	VORTEX VALVES, PRESS. RECOVERY BLEED — 8.9% INLET WT.	0.56
	COWL DOORS — 23% INLET WT.	1.50
	P INLET ADVANTAGE	2.06

Fig. 8 Cruise range advantage, P − N_5.

entire control margin. For the P inlet the operating point is at a lower pressure recovery of 90.3% but requires only 5.7% bleed mass-flow ratio. When the terminal shock wave moves upstream the bleed flow increases 0.022 and pressure recovery increases 0.029, providing the 5% decrease in engine-face corrected weight flow. The operating point distortion for the N_5 inlet is 11% and 8% for the P inlet. The lower distortion for the P inlet is probably due to the vortex generators on the cowl which were not present on the N_5 inlet.

Equally important as the engine-face performance is the bleed performance, defined mainly by the plenum chamber pressure recovery. The higher the pressure recovery in each plenum the lower the drag penalty of the overboard bleed flow. Figure 5 shows the bleed mass-flow ratio and plenum chamber pressure recovery for each bleed compartment of the N_5 and P inlets at the cruise operating points. The slight difference (0.071 vs 0.067) in total bleed mass-flow ratio for the N_5 inlet from that shown in Fig. 4 results from the slight difference in local Mach number (2.65 vs 2.60). The table shows that the plenum pressure recoveries generally increase from the forward to the throat plenums as would be expected from the increased compression as the main-duct airflow approaches the throat. The lowest plenum pressure recovery occurs for the N_5 inlet scoop which, as will be shown later, contributes a relatively high drag penalty. In addition, it is assumed that all the momentum of the vortex valve leakage airflow in the thrust direction is lost.

Cruise Range Penalties

Using the data from Figs. 4 and 5 the drag penalties for each bleed flow, including the vortex valve leakage, can be estimated and converted to a cruise range penalty of a typical Mach number 2.7 supersonic transport with a 3500 naut mile range.‡ Figure 6 shows the range decrements for the N_5 inlet in percent of cruise range. Figure 7 shows similar decrements for the P inlet. Each bleed penalty as indicated on top of the bars, consists of full-expansion total-momentum loss that is primarily a function of bleed pressure recovery, and exit ramp drag that is primarily a function of the bleed exit ramp angle. A discussion of bleed exit ramp drag will be given later. For the N_5 inlet the scoop penalty is the largest single bleed penalty causing 2.02% loss in range. Even the penalty for leakage through the vortex valves is considerable at 0.76% even though the leakage mass-flow ratio is only 0.4%. In comparison this leakage penalty is as large as that for the throat bleed. The total bleed, leakage, and exit ramp penalties represent a 7.22% loss in cruise range. Furthermore, operating at an engine-face pressure-recovery less than ideal (92.8%) represents an additional loss in range of 4.87%. For the P inlet there is no scoop bleed penalty, but the forward centerbody bleed accounts for the same range penalty of 2.02%. The total bleed and exit-ramp penalty for the P inlet is 1.27% less than for the N_5 inlet (including leakage); however, the pressure-recovery penalty is 1.65% greater.

For a clearer comparison of the N_5 and P inlets, Fig. 8 shows the incremental range advantage of the P inlet. This relative increment corresponds to the range decrement of the P inlet (Fig. 7) minus the N_5 decrement (Fig. 6). A positive value indicates an advantage for the P inlet.

‡The cruise range decrements for each bleed flow were calculated using Fig. 26 of Ref. 4. The penalties shown in the figure were adjusted for the corresponding differences in bleed flow, plenum chamber pressure recovery, and ramp static pressure for each of the bleed regions. Cruise range decrements for less than ideal engine-face pressure recovery and for increments in weight were obtained from Fig. 1 of Ref. 4.

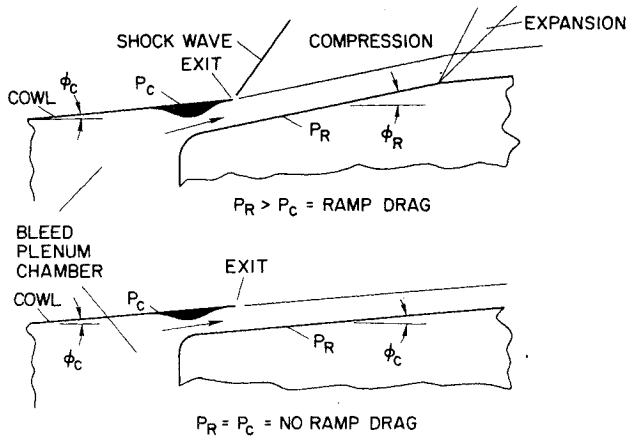

Fig. 9 Cowl ramp drag.

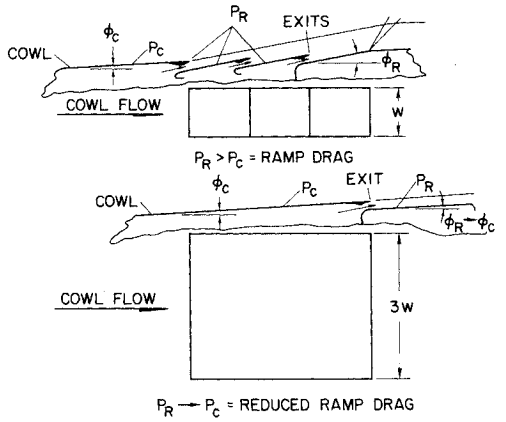

Fig. 10 Centerbody ramp drag.

The advantage gained by the P inlet which does not use a scoop or vortex valves is negated by the disadvantages of the remaining bleed penalties and the lower operating point pressure recovery. However, a smaller and therefore lighter inlet results from sizing the P inlet for lower bleed flow rate and lower pressure recovery and the elimination of the vortex valves. In addition the throat doors, which account for approximately 23% of the N_5 inlet weight and represent 1.5% loss in cruise range, are also eliminated. The net range advantage for the P inlet is then 2.06%.

Improved Performance

Exit Ramp Drag

As previously mentioned, the bleed exit-ramp drag can be a considerable part of the total bleed drag. Since the ramp drag is defined as the force arising from ramp pressures greater than the local cowl surface pressures, the ramp drag may be eliminated simply by reducing the ramp angle for the cowl and centerbody exits as shown in Figs. 9 and 10, respectively. The upper parts of Figs. 9 and 10 illustrate how ramp drag is developed, and the lower parts, how the ramp drag can be reduced or eliminated. For the cowl ramp (see Fig. 9), by reducing ϕ_r to ϕ_c the ramp drag can be eliminated since for a fully expanded flow the exit pressure equals the back pressure ($p_r = p_c$). However, making ϕ_r equal to ϕ_c creates a step in the cowl outer contour for each exit instead of the relatively smooth contour using the exit ramp. It might be argued here that it may not be possible to make $\phi_r = \phi_c$ because the net cowl angle may have to be increased for the same inlet length when the outer cowl contour is refaired from the cowl lip to the same maximum nacelle diameter.

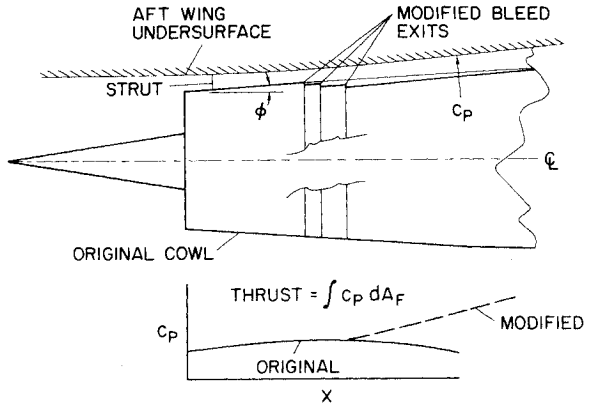

Fig. 11 Cowl interference.

Calculations for the P inlet indicate that refairing from an exit step area that accommodates fully expanded cowl bleed flow increases the cowl angle, thereby increasing the cowl drag value to approximately one half that of the eliminated ramp drag. However, for an aft underwing location of the nacelle, proper refairing of the nacelle and wing may yield enough favorable interference drag to overcome the drag increase due to increased cowl angle resulting from the refairing. Interference drag will be examined in more detail in the next section.

The ramp drag for the centerbody bleed exit louvers (see Fig. 10) arises from the cascade of ramps. In this case the ramp drag cannot be eliminated in the same manner as the cowl ramp drag since the louvers are restricted to a specific number of sectors equally spaced around the circumference. However, the drag can be reduced by spreading the exit area over a greater circumference as illustrated in Fig. 10 so that ϕ_r approaches ϕ_c.

Nacelle-Wing Interference Drag

If the greatest advantage is to be taken of the flowfield generated by the nacelle, it must be properly located to create a favorable interference flowfield between the nacelle and the airframe. The most likely location is on the aft portion of the underwing surfaces as shown in Fig. 11. The aft wing pressures are increased when the nacelle flowfield is imposed on the upward-sloping trailing edge of a typical warped and twisted supersonic wing planform. The farther aft the nacelle compression-flowfield pressures are the more beneficial the interference flowfield may be in reducing the wing drag. This is because a greater portion of the affected frontal area of the aft wing curvature may be exposed to greater nacelle compression flowfield pressures. By eliminating the ramp angle for each exit the rise in nacelle angle can be delayed to a further-aft nacelle station, increasing the wing pressure where it may be more beneficial as indicated by the dotted curve in the c_p vs x plot in the lower part of Fig. 11.

Short Subsonic Diffusers

One possible way to increase the cruise range is to reduce the inlet weight by shortening the subsonic diffuser. Figure 12 illustrates how this may be accomplished. Using the P inlet as a reference, the subsonic diffuser can be shortened to create a P_1 inlet, by bulging the cowl internal contour just ahead of the engine face to accommodate centerbody support struts with shorter chords but greater thickness. (The greater thickness will allow the same amount of centerbody bleed flow to exit through the shorter chord struts.) This scheme allows the inlet length (from the cowl lip to the engine face) to be reduced 14.3% from 2.45 to 2.1 diam, D.

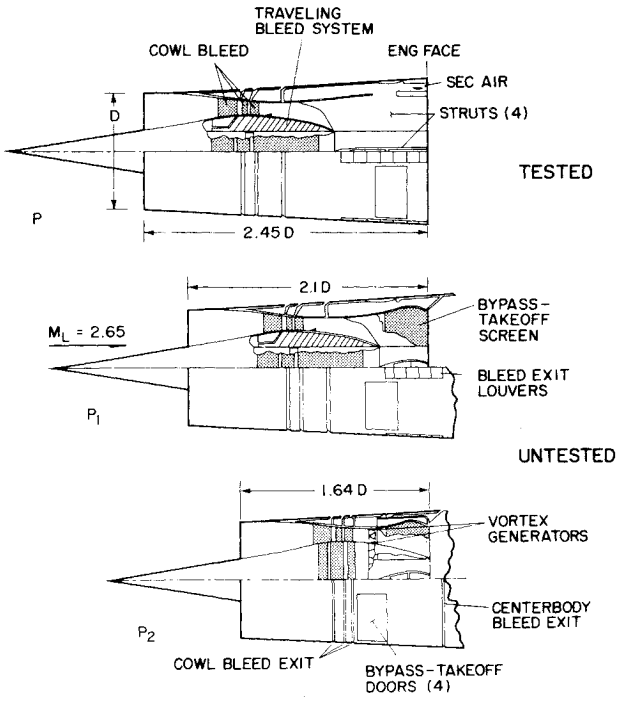

Fig. 12 Short subsonic diffusers.

Further reductions in inlet length can be accomplished by redesigning the supersonic diffuser with an increased centerbody diameter so that the throat remains fixed on the centerbody as it is translated for off-design operation. Redesigning eliminates the need for a traveling centerbody bleed system and in turn allows the struts to penetrate the aft section of the centerbody without disturbing a traveling bleed system. The cowl is also bulged to accommodate the thicker struts, as for the P_1 inlet. This much more speculative inlet design designated P_2, is illustrated in Fig. 12. The P_2 inlet is only $1.64D$ long or 33% shorter than the P inlet. In terms of cruise range, the reduced weight of the P_1 inlet increases the range approximately 1% over the P inlet, and the P_2 inlet further increases the range to 2%.§ However, the shorter inlets have higher cowl angles and therefore higher cowl pressure drags. This adverse effect counteracts to some extent the gain realized through reduced inlet weight. That is, an assessment of the changes in cowl pressure drag, skin-friction and aerodynamic interference of the nacelles on the wing of a typical transport indicates that the range improvement gained through lower inlet-weight will be reduced by approximately one half. This adverse effect may also be counteracted because reduced inlet weight will reduce the structural weight of the vehicle.

Cruise Range Improvement

Although the range improvement attributable to each item of inlet performance or weight is relatively small, the sum of all the improvements can be substantial. The following improvements believed achievable for the P_1 inlet compared to the P inlet are shown in Fig. 13:‡

	RANGE, percent
• ENGINE-FACE PRESSURE RECOVERY	1.7
• BLEED PRESSURE RECOVERY	1.0
• COWL BLEED EXIT LOUVER DRAG	1.3
• CENTERBODY BLEED EXIT LOUVER DRAG	1.9
• SHORT SUBSONIC DIFFUSER	1.0
TOTAL CRUISE RANGE IMPROVEMENT	6.9

Fig. 13 Cruise range improvement, P to P_1 inlet.

1) It is believed that the operating engine-face pressure recovery can be improved to approximately that of the N_5 inlet (2.5%) without increasing the operating bleed mass-flow ratio (5.7%). This can be accomplished by increasing the P inlet throat bleed system and/or using vortex or fast acting valves to achieve the required control margin. Assuming no weight and leakage penalties since these are small numbers, improved pressure recovery can contribute 1.7% increase in cruise range.

2) It should be possible to increase the bleed pressure recovery to that of each of the corresponding N_5 bleed plenum chambers. This increase in bleed-pressure recovery can be obtained by slanting all the P_1 inlet bleed holes forward 20° (relative to the local surface) except for the holes in the cowl throat which must be normal if adequate control margin is to be maintained (see "Inlets" section). This bleed-pressure-recovery improvement can account for 1.0% improvement in range.

3) Eliminating the cowl bleed ramp drag and

4) the centerbody bleed ramp drag can account for 1.3 and 1.9% improvement, respectively, assuming the increased cowl drag, as mentioned previously, can be recovered through favorable interference.

5) The shorter length of the P_1 inlet can account for another 1.0% if it is assumed that the adverse affects of increased cowl drag are counteracted by reduced vehicle structural weight because of the reduced inlet weight. The total cruise range improvement is then 6.9% (240 naut mile for 3500 naut mile range aircraft).

The range improvements shown are for a 633 lb/sec afterburning turbojet.[4] Current advanced supersonic transport studies[6] indicate that an engine with 50% more sea-level airflow may be required to meet the required sideline noise levels. This means that instead of a 6.9% increase in range from improved inlet performance, approximately 10% improvement for the advanced vehicle may be possible.

Conclusions

The results from wind-tunnel tests of two large-scale high performance axisymmetric inlet systems suitable for supersonic transports were studied. From these results a detailed evaluation has been made of the penalties, in terms of vehicle cruise range, boundary-layer bleed, airflow leakage, less-than-ideal engine-face pressure recovery, bleed exit-ramp drag, and inlet weight. Improvements in the inlet design were suggested to increase the cruise range of a typical long-range supersonic transport. Results indicate that improvements in design can increase the engine-face and boundary-layer-bleed pressure recoveries, reduce cowl and centerbody bleed exit ramp drag, reduce subsonic diffuser length (weight), and increase the favorable nacelle-underwing interference. Careful attention to each design detail can lead to a substantial improvement in range of approximately 6.9%. Furthermore, because of noise considerations future engines for advanced vehicles may be approximately 50% larger than used for the present study, making the effects of improved inlet performance even more important.

§Shorter subsonic diffusers may reduce the engine-face performance resulting in some range loss especially for the P_2 inlet. However, tests[5] of inlet systems with similar very short subsonic diffusers indicate that performance as high as for longer diffusers can be achieved.

‡No comparison with the P_2 inlet is made here because no detailed tests confirming the P_2 internal performance have been undertaken.

References

[1]Syberg, J. and Koncsek, J. L. "Transonic and Supersonic Test of the SST Prototype Air Intake," FAA-SS-72-50, April 1972, Federal Aviation Administration, Washington, D. C.

[2]Koncsek, J. L. and Syberg, J., "Transonic and Supersonic Test of a Mach 2.65 Mixed-Compression Axisymmetric Intake," CR 1977, March 1972, NASA.

[3]Smeltzer, D. B. and Sorensen, N. E., "Analytic and Experimental Performance of Two Isentropic Mixed Compression Axisymmetric Inlets at Mach Numbers 0.8 to 2.65," TN D-7320, June 1973, NASA.

[4]Tjonneland, E., "The Design, Development and Testing of a Supersonic Transport Inlet System," Paper 18 presented at the NATO/AGARD 38th Meeting of Propulsion and Energetics Panel, Sandefjord, Norway, Sept. 1971.

[5]Sorensen, N. E., Smeltzer, D. B., and Cubbison, R. W., "Study of a Family of Supersonic Inlet Systems," *Journal of Aircraft*, Vol. 6, No. 3, May–June 1969, pp. 184–188.

[6]Whitlow, J. B., "Comparative Performance of Several SST Configurations Powered by Noise Limited Turbojet Engines," TM X-68178, Dec. 1972, NASA.

MAY 1974 J. AIRCRAFT VOL. 11, NO. 5

Arbitrary Pressure Gradient Integral Technique for Predicting Boundary Layer and Thermal Parameters

Richard J. Flaherty*
United Aircraft Research Laboratories, East Hartford, Conn.

A new nonequilibrium eddy viscosity model, based on an equilibrium eddy viscosity correlation and a turbulent energy balance, is used within an integral procedure to describe transport properties in turbulent boundary layers. In the analysis, velocity and temperature profiles are represented by conventional power laws with variable power law exponents which are determined from correlations of mass entrainment associated with both the momentum and thermal boundary layers. Stanton number is determined as a function of the Reynolds stress near the wall (but outside the influence of the laminar sublayer) and the shapes and relative sizes of the velocity and thermal boundary layers.

Nomenclature

C_f = wall friction coefficient, $\tau_w/(\frac{1}{2}\rho_e u_e^2)$
C_f' = peak Reynolds stress coefficient near the wall, $\rho_w\overline{u'v'}/(\frac{1}{2}\rho_e u_e^2)$
C_p = specific heat at constant pressure
H = δ^*/θ
H_i = $1 + 2n$
H_m = $1 + 2m$
k = thermal conductivity
M = Mach number
m = temperature profile exponent, $(T_t - T_w)/(T_{te} - T_w) = (y/\delta_h)^m$
n = velocity profile exponent, $u/u_e = (y/\delta)^n$
n_w = $rC_f'/0.14 + [(rC_f'/0.14)^2 + (rC_f'/0.14)]^{1/2}$
n^* = eddy viscosity parameter
P_r = laminar Prandtl number, $\mu C_p/k$
P_{rt} = turbulent Prandtl number (assumed to be 0.9)
P_{t_t} = total pressure at edge of boundary layer
$\bar{R}_h$ = weighted resistance, thermal
$\bar{R}_u$ = weighted resistance, momentum
r = $1 + [(T_{te}/T_e)^{1/2} - 1]\, e^{-0.02/\mathrm{In}1/3.1}$
S_T = Stanton number
s = surface distance
T = temperature
t = time
u = velocity
u' = turbulent velocity component in the flow direction
v' = turbulent velocity component normal to the wall
W = velocity boundary layer mass thickness, $\int_0^\delta \rho u/\rho_e u_e\, dy$
W_h = thermal boundary layer mass thickness, $\int_0^{\delta_h} \rho u/\rho_e u_e\, dy$
y = distance normal to wall
y^+ = $(\frac{1}{2}\rho_w\rho_e^2 C_f')^{1/2} y/\mu_w$
γ = ratio of specific heats
δ = velocity boundary-layer height
δ^* = boundary-layer displacement thickness
δ_h = thermal boundary-layer height
ϵ = kinematic eddy viscosity
Θ = momentum deficity thickness, $\int_0^\delta \rho u/\rho_e u_e(1 - u/u_e)\, dy$
μ = viscosity
τ = shear
ϕ = thermal energy deficity thickness, $\int^{\delta_h} \rho u/\rho_e u_e(1 - T_t/T_{te})\, dy$

Subscripts

aw = adiabatic wall
e = edge of the boundary layer
t = total (stagnation) conditions
w = wall
p = heat transfer reference point in the boundary layer ($200\, y^+$)
ref = Eckerts reference temperature

Presented as Paper 73-700 at the AIAA 8th Fluid and Plasma Dynamics Conference, Palm Springs, Calif., July 16–18, 1973; submitted August 20, 1973; revision received February 28, 1974.

Index category: Boundary Layers and Convective Heat Transfer—Turbulent.

*Senior Research Engineer.

Introduction

A PHYSICAL description of an integral method for predicting laminar and turbulent boundary-layer growth and heat transfer is presented. In this method the von Kármán boundary-layer momentum integral equation is numerically integrated in the streamwise direction using auxiliary equations to compute the form factor and skin friction. Velocity and temperature profile shapes needed for the analysis are determined from mass entrainment models which utilize a new nonequilibrium eddy viscosity formulation for turbulent flow situations.

The present entrainment method, developed to fulfill a need for a simple-to-use, yet accurate and fast boundary-layer predictive scheme, has been applied successfully to